

AN ALTERNATE FINE GUIDANCE SENSOR FOR THE SPACE TELESCOPE

A study was conducted to develop a preliminary design of an alternate fine guidance sensor for the National Aeronautics and Space Administration's Space Telescope; an electrostatically focused silicon diode, quadrant array detector was selected. Simulations of the Space Telescope control system showed that the recommended sensor could meet the required performance specifications and would be substantially more robust than the baseline design that used a Koesters prism interferometer. Configuration studies verified the feasibility of retrofitting the sensor into the existing spacecraft.

INTRODUCTION

The National Aeronautics and Space Administration's Space Telescope (Fig. 1) will be the largest spacecraft ever orbited for the purpose of making astronomical observations. Intended to be deployed by the space shuttle into a 600-kilometer-altitude circular orbit, it will be 13 meters long and weigh over 11,000 kilograms. Its 2.4 meter primary mirror rivals all but the largest earth-based instruments in light-gathering power. With the ability to make extremely long exposures that are not possible from the ground, the Space Telescope's sensitivity will be substantially greater than that of any existing telescope. Because of its ability to operate outside the atmosphere, its effective resolving power of 0.1 arc-second exceeds that of any ground-based telescope. The Space Telescope will enable astronomers to see farther and with greater detail than with any previously available instrument.

Full utilization of the capabilities of the Space Telescope requires the design of a spacecraft pointing control system that yields greater accuracy and stability than have been required for any previous mission. A pointing accuracy of 0.01 arc-second is needed so that spacecraft pointing errors will not contribute significantly to overall image degradation. To achieve the long exposures necessary to bring out details in very faint sources, the telescope must hold its position to within 0.007 arc-second over a 24 hour period. So that astronomers may study sources in the distant universe, many observations must be made toward the galactic poles, away from crowded regions containing many stars. This in turn implies that very dim, 14.5 visual magnitude stars must be used as reference sources for telescope guidance. The task, which is accomplished by a spacecraft subsystem called the fine guidance system, is comparable to hitting a bullseye the size of a twenty-five-cent coin in Boston with a bullet from a rifle in Washington while deriving one's sighting information from sources 2500 times too dim to be seen by the human eye.

Thus, the development of a suitable fine guidance system for the Space Telescope is extremely challenging. Early in the program it was decided to implement a scheme based on the use of a Koesters prism interferometer, which is used by astronomers to resolve binary stars that are separated by very small angular distances and thus has the potential for very high angular resolution. However, its use as part of an operational attitude control system for a spacecraft has not been demonstrated, and many difficulties were encountered in its design and fabrication. The principal problem with the interferometric fine guidance system was its relatively limited useful angular range of approximately ± 0.04 arc-second. The concern was that disturbances resulting in telescope jitter or boresight shifts outside that range could cause loss of fine lock on the guide stars, thus ruining the observation in progress.

In 1983, The Johns Hopkins University developed a preliminary design for an alternate fine guidance sensor for the Space Telescope. The alternate sensor was required to demonstrate an accuracy and sensitivity adequate for the telescope's scientific requirements while exhibiting a much larger angular dynamic range, and hence a more forgiving performance characteristic, than the interferometric system. Within these constraints, the "best" design was considered to be one that would have the least impact on the Space Telescope program should conversion to an alternate sensor be required. It should be conceptually and operationally simple, pose reasonable requirements for integration into the present spacecraft design, and introduce minimum cost and schedule perturbations into the program.

Various alternate sensor concepts were studied, including enhancements to the basic Koesters interferometer and alternate sensor devices such as image dissectors, charge-coupled or charge-injection devices, microchannel plates, optical image splitters, and electrostatically focused quadrant detectors.¹ A premium

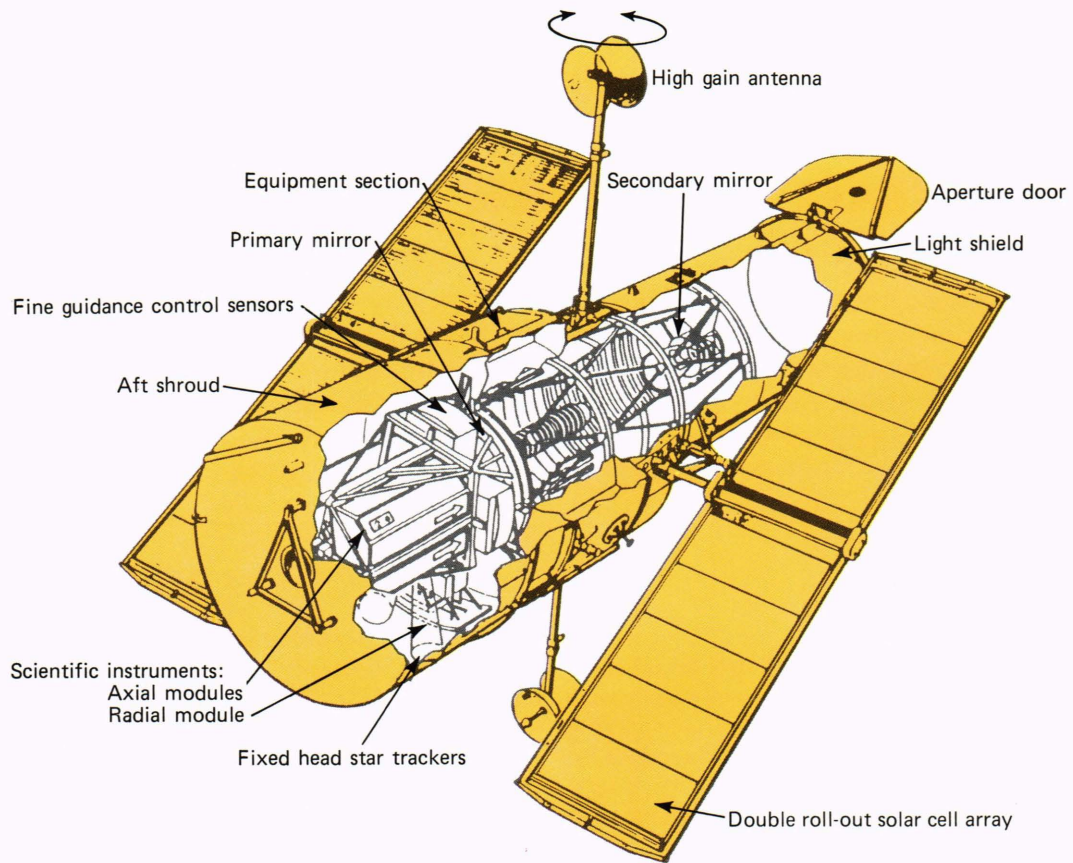


Figure 1—Configuration of the Space Telescope.

was placed on performance verification through measurements. Based on available data, the electrostatically focused Digicon (marketed by the Electronic Vision Systems Division of Science Applications, Inc.) is the sensor that best fits the guidelines and constraints appropriate to a retrofit design.

SPACE TELESCOPE OBSERVATORY

The Space Telescope uses a standard and conceptually simple attitude determination and control system and is three-axis-stabilized in inertial space to facilitate astronomical observations. Reaction wheels provide control torques for both large-angle reorientations and small error-correction maneuvers. Accumulation of angular momentum in the wheels due to both secular and large-amplitude cyclic disturbance torques is avoided by using magnetic torquer bars that act continually to remove angular momentum. The closed-loop attitude control uses a rate gyro assembly for direct sensing of angular motion, with positions obtained by integrating the rate data. For coarse control, standard fixed-head star trackers provide an inertial reference. The fine guidance system fulfills the same function during science observations.

The optical system consists of a reflecting telescope of the Ritchey-Chretien design with a 2.4-meter primary mirror and a 57.6-meter focal length, which provides an $f/24$ system. This arrangement gives a usable field of view 28 arc-minutes in diameter that is shared

by five science instruments and three identical fine guidance systems. Since only two of the fine guidance systems are needed for pointing control at any one time, the unused instrument is available for astrometry measurements, thus making it effectively a sixth scientific instrument. The division of focal plane light is shown in Fig. 2.

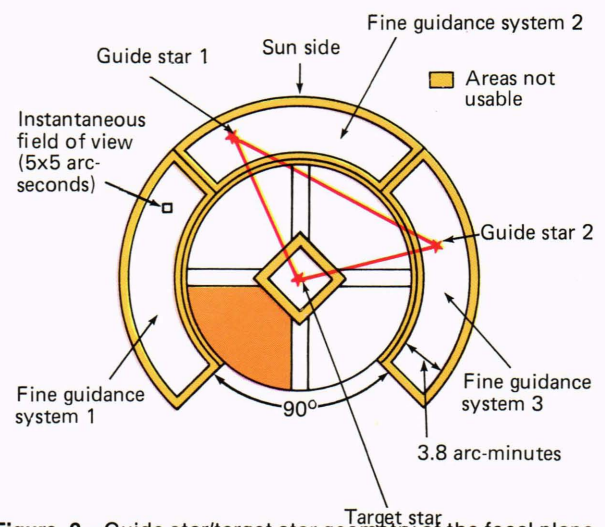


Figure 2—Guide star/target star geometry of the focal plane light.

Each fine guidance system receives light from a segment of the focal plane extending radially from 10 to 14 arc-minutes and axially over a 90° arc, for a total focal plane area of 69 square arc-minutes. The region is optically degraded by astigmatism and other aberrations, and corrector elements must be used in the optical train of the fine guidance system optics prior to the interferometer. The entire field of view is scanned mechanically by a 5 arc-second-square pupil both during guide star acquisition, when the total field of view must be searched for a particular star, and during fine lock, when active scanning is used to keep the guide star near the center of the useful range of the interferometer. Figure 2 shows the 5 arc-second-square instantaneous field of view in relation to the total fine guidance system field of view.

ALTERNATE SENSOR CONCEPT

The Digicon sensor requires the formation of a real star image and the focusing of that image on the sensor. In this it is different from the interferometer, which operates with input that is a spatial Fourier transform of the real image. The block diagram for the interferometer system is shown in Fig. 3, while that for the Digicon sensor is shown in Fig. 4.

The optical elements in Fig. 4 are shown schematically in Fig. 5, which depicts the recommended alternate sensor configuration. All optical elements before the beam splitter in the present system are retained in

the new design. They serve to remove the aberrations present in the off-axis regions of the focal plane from which guide star images are obtained. The focal plane is also scanned by the optical elements in conjunction with the star selector servomechanisms. The corrected star image quality is sufficient for fine guidance purposes in the recommended mode of operation.²

The relay optics needed to form an image were not required for the interferometer; a design for a small Cassegrain telescope to perform this function was developed by David Grey Associates.²

QUADRANT DETECTION

The Digicon can produce an error signal of the type (shown in Fig. 6) that has an essentially linear range about a region near the origin and a nonlinear transition to a limiting value of ± 1 far from the null position. This high limiting signal contrasts with the nominal Koesters interferometer characteristic, shown in Fig. 7, which returns to a low signal limit at large displacements. Large boresight displacements thus yield the same error signal as small pointing errors, a potentially confusing situation.

The advantages for control system design using the error signal of Fig. 6 are obvious. If the system is perturbed to, or is initially at, a position far from the desired null, appropriate directional information for error correction is still obtained. This permits a control scheme to be developed that is of a classical "bang-

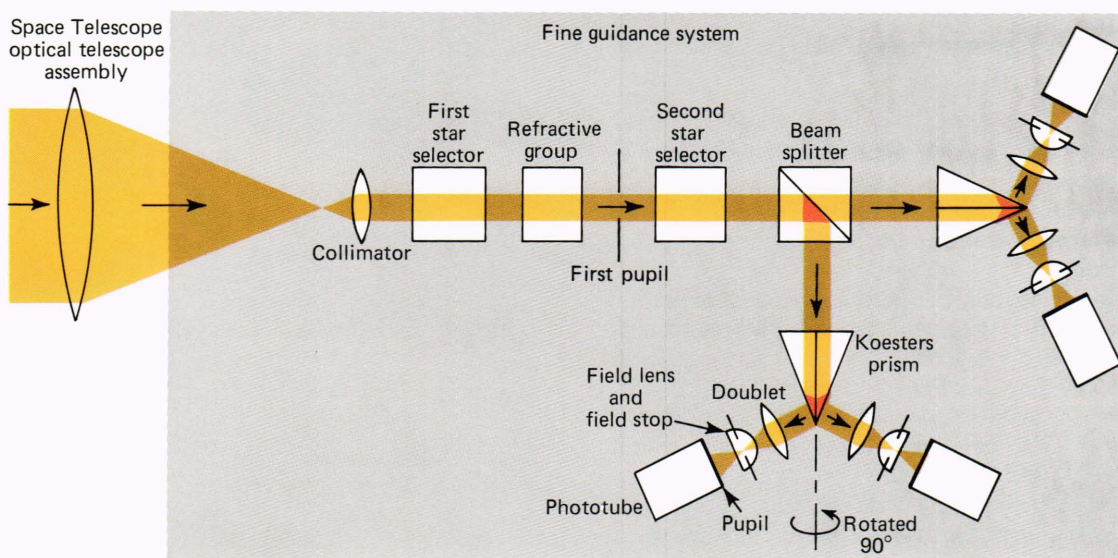


Figure 3—Block diagram of the Koesters prism interferometer.

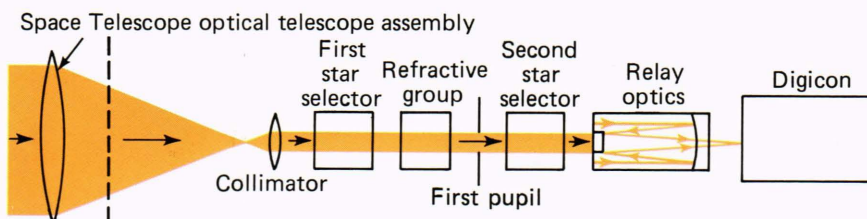


Figure 4—Block diagram of the Digicon alternate sensor.

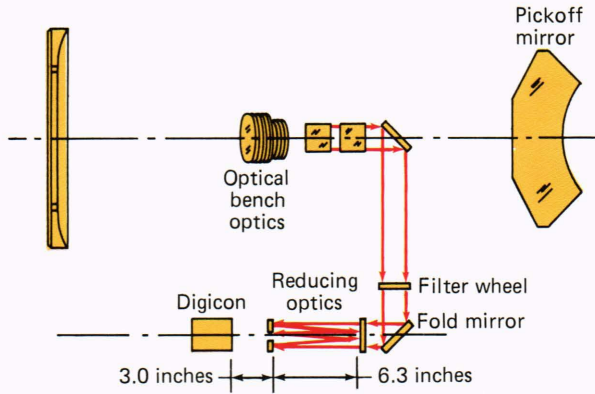


Figure 5—Schematic drawing of the optical elements of the Digicon alternate fine guidance system.

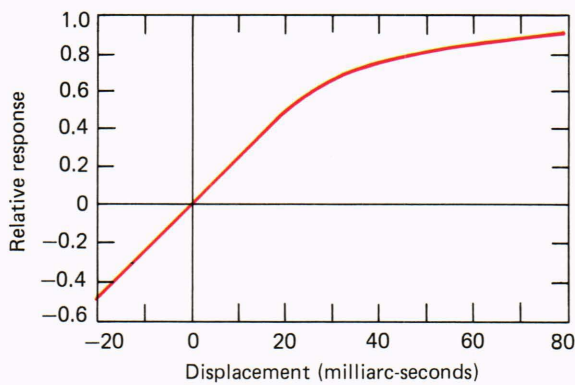


Figure 6—Theoretical error characteristic of the optical splitter.

bang” form far from the origin and that provides a response proportional to the error near the origin, allowing good performance in fine lock while providing robust behavior in the presence of major disturbances.

With the devices considered here, the desired error-response function is obtained by means of the so-called quadrant detector mode of operation. The input field of view in the fine guidance system is 5 arc-seconds square and is assumed to contain one guide star in the desired 10 to 14.5 visual magnitude range. The small instantaneous field of view must be scanned over the larger, 69 square-arc-minute field available to each fine guidance system in order to find a potential guide star. (Statistical analysis yields a greater than 95 percent probability that such a guide star will be present.) The input signal is divided either optically or electronically into four quadrants, as shown in the inner group of elements in Fig. 8. The star image diameter should be large with respect to the array gaps.

If we consider the signal S defined by

$$S = \frac{(A + B) - (C + D)}{A + B + C + D}, \quad (1)$$

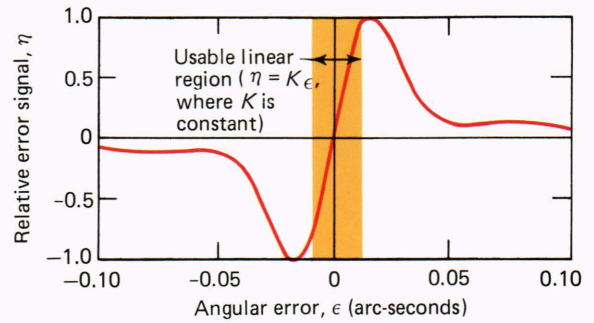


Figure 7—Gain characteristic function of the Koesters prism interferometer.

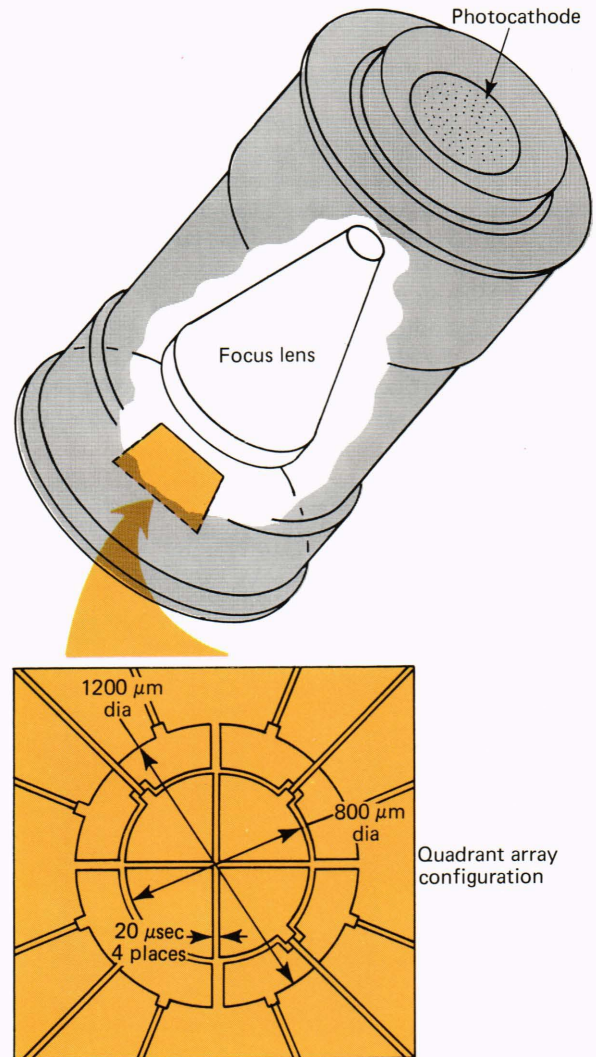


Figure 8—The quadrant Digicon.

where A , B , C , and D are the separate signals from the four inner quadrants, several results are evident. First, the denominator is the total signal and serves as a normalizing factor that remains constant as long as the star is in the field of view. Second, the numerator represents the signal difference between the upper and lower halves of the detector array and thus is zero

if the star image is centered with respect to the horizontal gap. If it drifts partly above the line, the numerator will be positive, and if it drifts below the line, the numerator will be negative. If the image is entirely above the horizontal split, $C + D = 0$ and $A + B = A + B + C + D$, so that $S = 1$. Thus, S is an error signal that is zero if the image is centered and unity if it is displaced a large distance above the centerline, exactly as shown in Fig. 6. The width of the linear range and the nature of the transition to the limiting values of ± 1 depend on the image characteristics and the size of the image relative to the gaps.

Clearly, the same operation can be performed with the left and right halves of the detector array, and the two error signals thus available can be used to center the image in the field of view. Note that if more than one star is present, the scheme is still viable because the algorithm merely works to bring the optical centroid of the stars in the field of view to the center of the array. This has advantages if, as may happen, a selected catalog guide star is in fact an unsuspected binary.

DIGICON CHARACTERISTICS

The electrostatically focused Digicon is a structurally and operationally simple device. Test results show the capability for uncooled operation with 14.5 visual magnitude guide stars with noise equivalent angles in the 0.003 to 0.004 arc-second range. The Digicon operates by electrostatically accelerating electrons emitted from a photocathode, after which they hit a silicon diode detector array, generating hole-electron pairs at the rate of 1 pair per 3.6 electronvolts of photoelectron energy. Since an accelerating potential on the order of 16 kilovolts is used, several thousand electrons per photoelectron are ultimately collected and amplified. The pulses produced occur at a low enough rate (less than 100,000 per second) for counting of individual pulses (i.e., photon counting) to be performed. Figure 9 shows the basic Digicon device together with a

diode array appropriate for a guidance application similar to that for the Space Telescope.³ Inner/outer diode clustering, as shown in Fig. 8, allows a wide (5 arc-second) field of view for acquisition, yet permits a narrow (e.g., 0.5-arc-second) field of view for fine lock, reducing sensitivity to background noise and extraneous stars and having advantages for astrometry as well as for guidance.

The electrostatic Digicon is inherently susceptible to deflections of the focused beam by stray magnetic fields. Tests revealed that the unshielded Digicon shown in Fig. 7 yielded a beam deflection in the Space Telescope magnetic field environment of approximately 0.4 arc-second, assuming use of an $f/24$ imaging system. A reduction in sensitivity by a factor of 1000 or more is required and can be obtained as shown in Fig. 9, where the Digicon is surrounded by two layers of shielding separated by $\frac{1}{4}$ inch or more. Tests show that a single shield provides an attenuation factor of roughly 60. Separation of the shielding layers produces a cascade effect and a total attenuation of several thousand. Use of higher f -number imaging systems, as proposed, would reduce the angular sensitivity even further.

An issue of primary importance during the study was the nature of the characteristic error function produced by the Digicon in response to angular deviations of the focused star image from the center of the quadrant diode array. While having the general form of Fig. 6, it is important that the slope of the curve in the linear response region be as high as possible. Also, some concern existed as to whether the gaps in the diode array would be large enough to cause an appreciable number of photons to be lost. The two Digicon characteristics that require the most study to resolve these issues are the edge response of the diodes and the beam spread between the photocathode and the diode array.

Tests were conducted⁴ by scanning a small (4 to 5 micrometer) spot of light across the Digicon photocathode (coulomb spreading produces a larger im-

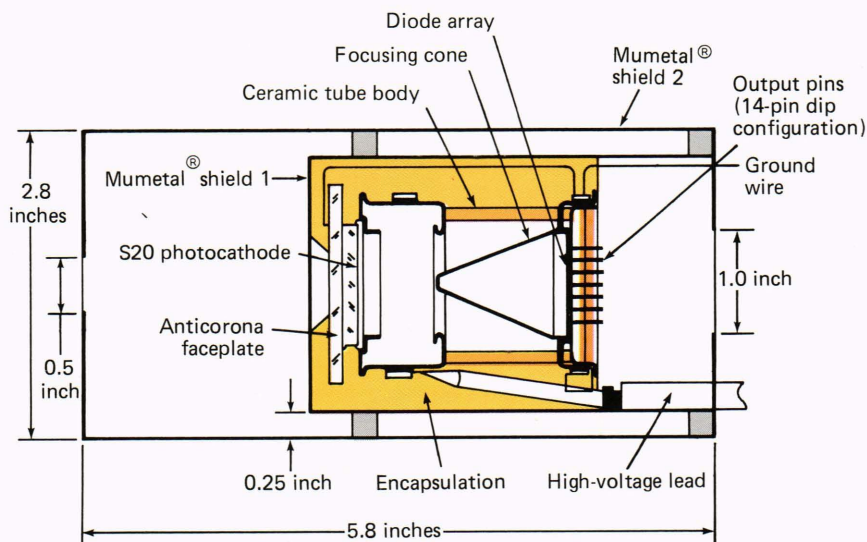


Figure 9—Encapsulation and magnetic shielding of the internal components of the Digicon.

age on the diode array) and measuring the counts from the various diodes as a function of spot position. The tube was a quadrant Digicon with an outer guard ring having the geometry shown in Fig. 8. All scans were made in the inner quadrant array. Parameters that varied from scan to scan included the diode bias and the discriminator threshold setting as a percentage of single-electron pulse height (the parameter that determines whether an individual photoelectron is "seen" by the counting circuitry).

The pulse height distribution from a typical Digicon is given in Fig. 10. The discriminator threshold is a level determined by a vertical line set to the left of the peak of the distribution. Moving the threshold to the left increases the number of pulses with "substandard" (relative to the single-electron peak) amplitudes that are counted. Photoelectrons striking the gap area ionize material. Some of the electrons produced are collected in each diode, thus appearing as substandard pulses. By lowering the threshold, more pulses are counted, effectively narrowing the gap. The effective "edge" of the gap was defined as the point where the signal collected was reduced by 50 percent from its maximum value in the middle of the diode.

Spot scans across a gap with a geometrical width of 15 micrometers in regions removed from the center showed effective gap widths ranging from 10.4 micrometers with a 70 percent discriminator threshold to 2.6 micrometers with a 40 percent threshold. Scans across the center (where the geometrical gap is wider due to rounding of the diode corners) yielded widths of 21.2 to 15.7 micrometers for the same threshold range. Variation of diode bias, for spot scans through the center of the array, indicated effective gap widths between 15.7 micrometers at 10 volts to 11.8 micrometers at 15 volts. Adjustment of diode bias and discriminator threshold can thus be used to control effective gap width; however, in no case does it appear that the effective gap width is grossly different from the geometrical gap width, nor that excessive attenuation results from photoelectrons lost in the gap. Di-

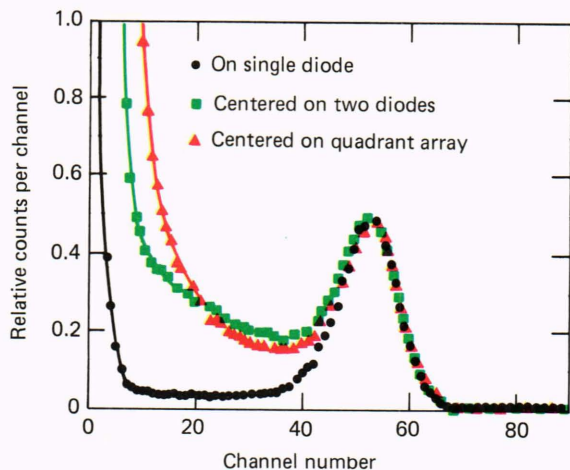


Figure 10—Digicon pulse height distribution for three cases. All distributions are normalized to the peak.

ode arrays with patterns suited to our purpose can be obtained with geometrical gap widths in the 3 to 7 micrometer range.

With these results, the Digicon characteristic error function was obtained by modeling the diode gaps as square well potentials 6 micrometers wide. An image profile representative of that for the Space Telescope optical system¹ was used to model the incident star image. A gaussian beam with a standard deviation spread of 12 micrometers was used to model the defocusing of photoelectrons between the Digicon photocathode and the diode array. An *f*/50 system was assumed; the resulting error function is shown in Fig. 11. As seen, it is nearly indistinguishable from the curve resulting for a perfect optical splitter (Fig. 6). Analysis shows that the Digicon sensor in conjunction with an *f*/50 or larger imaging system would yield a noise-equivalent angle of 0.003 to 0.004 arc-second at the 40-hertz sample rate of the fine guidance system.

ACQUISITION OF THE GUIDE STAR

As stated, the guide star acquisition process for the Digicon sensor is fundamentally different from that of the interferometer system so it was necessary to develop and verify a new transition mode controller for guide star acquisition.

For conceptual design and evaluation purposes, a simple dynamical model was used to represent the motion of the guide star in the detector field of view. A two-axis model using the position, velocity, and acceleration of the star was employed, and realistic constraints on image velocity and acceleration caused by star selector servo limitations were included.

The control law chosen for the transition mode was a modified bang-bang scheme, with state feedback used to enhance performance in the linear region of the Digicon characteristic error function. In order to implement the control law, estimates of star position and velocity are required. A simple observer (a suboptimal fixed gain Kalman filter) was constructed to produce those estimates from Digicon sensor and star

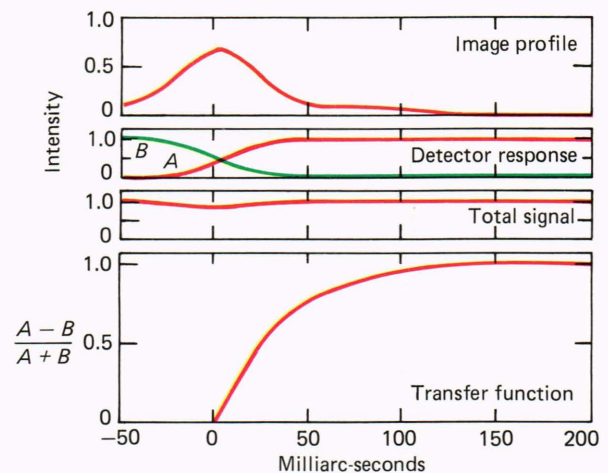


Figure 11—Transfer error function of the Digicon.

selector servo encoder output data. The observer and control law are discussed in more detail in Ref. 5.

Simulations and evaluations of the transition mode controller outlined above were carried out for a series of acquisition scenarios of varying difficulty. Figures 12, 13, and 14 show typical results. In these cases, the initial guide star velocity is at its maximum but varies in direction from case to case. Figure 13 is particularly interesting; the initial velocity of the guide star is such that the star temporarily leaves the detector field of view after initiation of the transition mode. However, the controller uses encoder-derived velocity information to continue driving the guide star position toward the origin. The double-star cases are also interesting; as is shown in Fig. 14, the controller centers the brighter star at the origin.

Guide star acquisition procedures with the Digicon sensor appear to be extremely efficient and robust. Transition from the search mode to the fine lock mode requires less than 2 seconds in all cases, compared with 30 seconds or more with the interferometer. This is true even for severe cases where the guide star temporarily leaves the field of view or where more than one star is present.

FINE LOCK PERFORMANCE

The theoretical advantage of the Koesters prism interferometer in the baseline fine guidance system is that very fine angular resolution is potentially available, which allows precise pointing stability. The Space Telescope specification is 0.007 arc-second (standard deviation) jitter for 24 hours with a 14.5 visual magnitude guide star. It was necessary to demonstrate that the alternate sensor design was capable of meeting that requirement. Such a demonstration can only be given via computer simulation of the spacecraft pointing control system, with the Digicon error response func-

tion used in place of the nominal Koesters interferometer response. Extensive use was made of models previously developed at both the Goddard and the Marshall Space Flight Centers. However, several features not present in either of these models but judged to be important were added during the course of the work. Only single-axis simulations were performed.

The simulation uses six rigid body structural modes and four selectable flexible body modes out of 280 available in the structural model. Associated with each of these modes is a natural frequency (0.08 to 70 hertz) and a damping ratio (typically 0.003 to 0.005) that are used in the assumed second-order transfer functions for each mode.

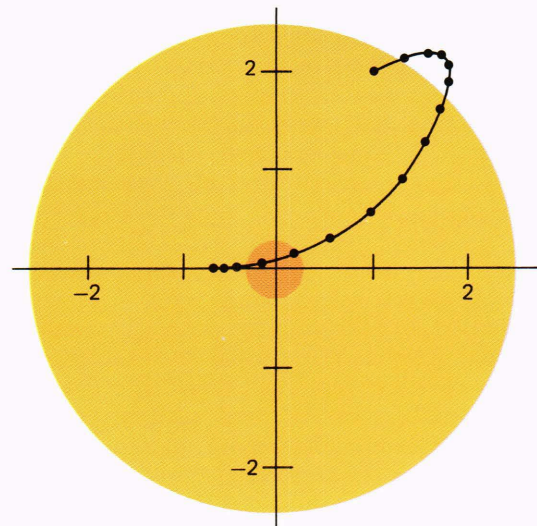


Figure 13—Simulation results for scenario 2. This case shows the robust behavior of the guide star acquisition algorithm. Notice how the star is ultimately centered in the field of view, even though its initial track takes it temporarily out of range.

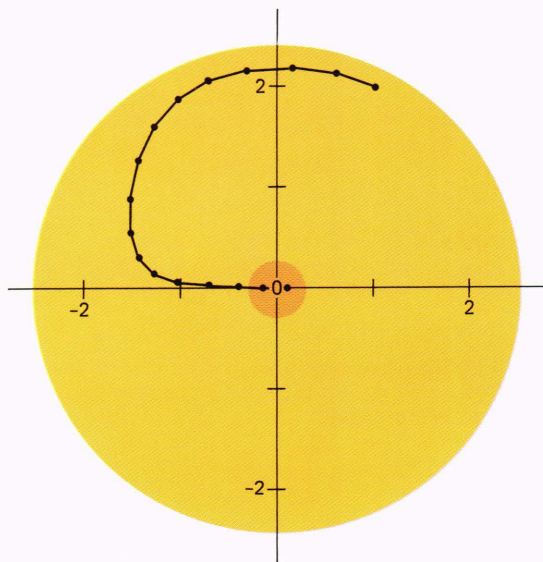


Figure 12—Simulation results for scenario 1, the basic guide star acquisition case, showing the ability of the Digicon sensor to center the star in the field of view.

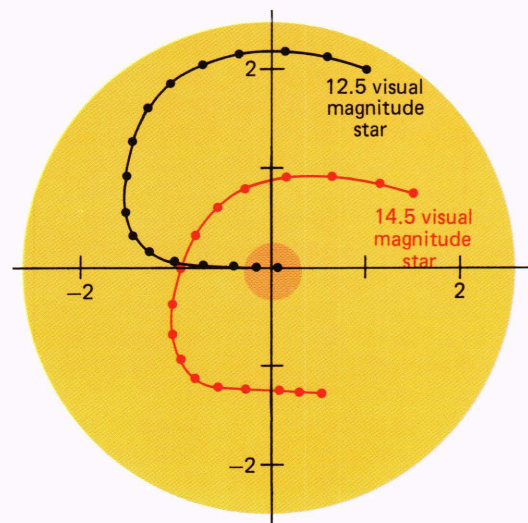


Figure 14—Simulation results for scenario 3. This case shows the behavior of the acquisition algorithm with two stars in the field of view. The sensor centers on the brighter star.

Three noise sources affecting the fine guidance system pointing stability are included in the model: guide star photon noise and position, and rate noise in the spacecraft rate gyros. Cubic spline interpolation of tabulated sensor data, determined either experimentally or analytically, is used to generate the sensor error characteristic.

Varied disturbance models were used in the simulation; they could be turned on either individually or in combination. They included

1. Cosmic ray strikes of selectable magnitudes at specified times;
2. Step-function boresight shifts of variable magnitude, used to simulate the effects of thermal “creaking” of the structure;
3. Axial forces, generated by the spacecraft reaction wheels, that can “pump” certain structural modes under some conditions;
4. Torque pulse disturbances emanating from the high-resolution spectrograph carousel and the wide-field/planetary camera shutter;
5. Disturbance torques due to high-gain antenna articulation.

Further details on the simulation model, including block diagrams, are included in Refs. 5, 6, and 7.

Results obtained from the simulation were very promising. Baseline operational and environmental scenarios were defined,⁶ and pointing stability was analyzed with both the Koesters prism interferometer and the electrostatically focused quadrant Digicon. Figure 15 shows the performance of each system in the baseline scenario. It is seen that the two sensors perform about equally well, with the Digicon results perhaps slightly better. Results such as these established that, on a one-to-one comparison basis, the Digicon alternate sensor was fully capable of meeting the Space Telescope jitter specification.

Of possibly greater interest is the behavior of each sensor system under the stress of random but realistic disturbances. Figure 16, the interferometer performance in the presence of a 0.06 arc-second thermal creak, shows that large pointing errors result. Figure 17 shows the Digicon performance with the same disturbance. Because of the different sensor error characteristics at large displacements, the Digicon system returns quickly to its nominal behavior, with only a small effect on the overall jitter.

Similar results were produced for disturbances caused by cosmic rays, science instrument induced torques, etc. In all cases, the Digicon system is as accurate in the steady state and more robust in the presence of disturbances than the interferometer.

Figure 18 demonstrates the robustness of the alternate sensor design in another way, by showing the decrease in system performance as a function of diminishing guide star brightness. It is seen that the Digicon retains lock (defined as the 0.007 arc-second pointing jitter level) out to stars of nearly 19 visual magnitude, while the interferometer fails at less than

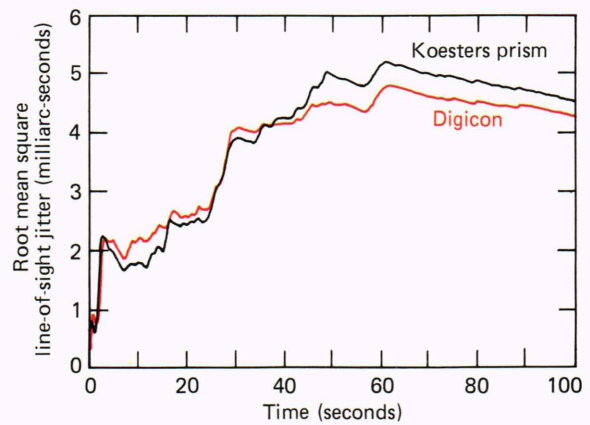


Figure 15—Baseline root mean square of scientific pointing error for the Koesters prism interferometer and the Digicon.

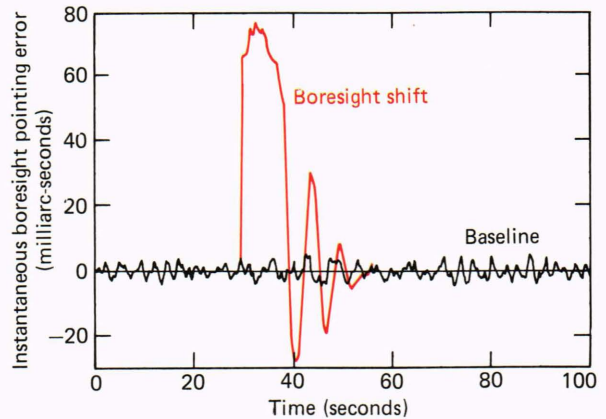


Figure 16—Fine guidance sensor pointing error for the Koesters prism interferometer; baseline design and boresight error were added.

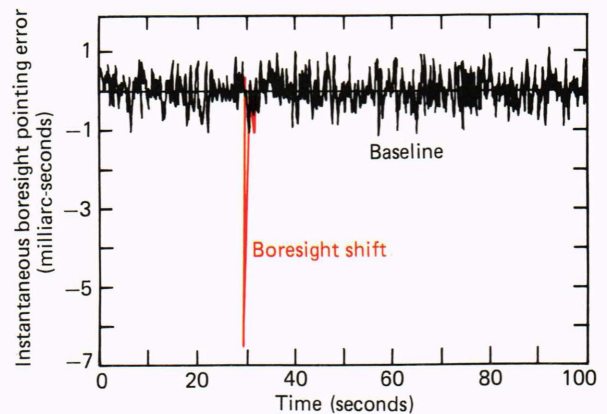


Figure 17—Fine guidance sensor pointing error for the electrostatically focused quadrant Digicon; baseline design and boresight error were added.

17 visual magnitude. While these results are indicative of the relative design margin in the two approaches, it should be noted that both systems are well within the required performance specifications.

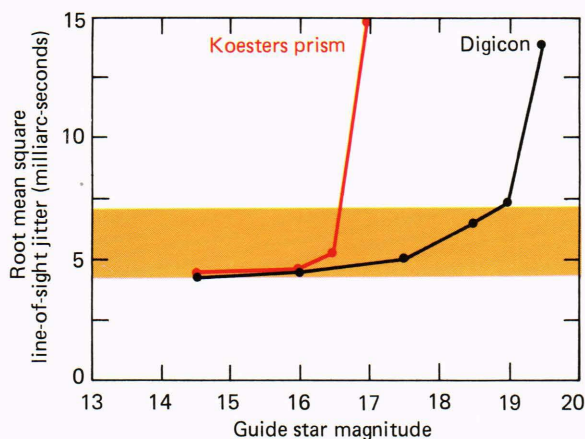


Figure 18—System performance versus guide star magnitude for the Koesters and Digicon systems.

CONCLUSIONS

The alternate fine guidance sensor program was initiated in response to concerns over the ability of the interferometric fine guidance sensor to meet its performance specifications and to function in a flexible and robust manner, in the presence of unforeseen, and perhaps unforeseeable, operational disturbances. The work reported here has shown that the electrostatically focused quadrant Digicon is an excellent candidate for an alternate sensor, capable of meeting the Space Telescope pointing performance goals with minimum technical risk and configuration impact. A feasible approach to integrating the Digicon sensor into the existing fine guidance system assembly has been developed, the availability of required new components has been demonstrated, and suitable versions of necessary new algorithms have been generated.

REFERENCES

- 1 M. D. Griffin, T. E. Strikwerda, and D. G. Grant, *Space Telescope System Study Report*, JHU/APL SDO 6941 (1983).
- 2 David Grey Associates, *Final Report Submitted to the Applied Physics Laboratory* (1983).
- 3 R. O. Ginavin, L. L. Acton, R. D. Smith, J. G. McCoy, D. G. Currie, and E. A. Beaver, "Performance of a Digicon Photon-Counting Autoguide System," *Proc. SPIE 8 Symposium on Photoelectric Image Devices*, London (Sep 5-9, 1983).
- 4 R. O. Ginavin, *Fine Guidance System Digicon Study*, final report Electronic Vision Systems Division, Scientific Applications, Inc. (1983).
- 5 M. D. Griffin, T. E. Strikwerda, and D. G. Grant, *Space Telescope Alternate Fine Guidance Sensor Design Study*, JHU/APL SDO 7083 (1983).
- 6 M. D. Foust and K. Strohhahn, *Performance Evaluation of the Koesters Prism Interferometer and Alternate Sensors for the Fine Guidance System of the Space Telescope*, JHU/APL SDO 7098 (1983).
- 7 A. J. Pue, *Description of the Space Telescope Three-Axis Control System and Some Single-Plane Analyses*, JHU/APL SDO 7043 (1983).

ACKNOWLEDGMENTS—This study was conducted by The Johns Hopkins University under the sponsorship of the National Aeronautics and Space Administration's Marshall Space Flight Center, with W. G. Fastie of The Johns Hopkins University as the principal investigator. The effort described here was carried out at APL under the direction of David G. Grant and is the product of the work of many staff members in addition to the principal authors. We take this opportunity to acknowledge the contributions of Tom Coughlin, Jay Dettmer, Michael Foust, Rob Gold, Gene Heyler, Bernard Hochheimer, Ben Hoffman, John Hunt, Doug Mehoke, Fred Mobley, Ted Mueller, Alan Pue, Courtney Ray, William Skullney, Kim Strohhahn, Ralph Sullivan, Joe Tarr, Charles Twigg, and Clarence Wingate. We also wish to acknowledge the assistance received from Sahag Dardarian and Michael Femiano of the Goddard Space Flight Center, and Gerald Nurre,

Hans Kennel, and Mike Polites of the Marshall Space Flight Center. We thank Charles Jones and John Humphreys of the Marshall Space Flight Center for their role in sponsoring this work. Terry Facey of Perkin-Elmer, Jack Rodden of Lockheed Missiles and Space Corp., Alan Goldberg of OAO Corp., and Doug Currie of the University of Maryland deserve our thanks for their assistance during the course of the program.

THE AUTHORS



MICHAEL D. GRIFFIN (left) is the program scientist for the Polar Bear satellite program. He was born in 1949 in Aberdeen, Md. He has received five degrees in physics, electrical engineering, and aerospace engineering from The Johns Hopkins University, Catholic University, University of Southern California, and University of Maryland. He is a Registered Professional Engineer in Maryland and is an Associate Fellow of the American Institute of Aeronautics and Astronautics.

Dr. Griffin is a member of the principal professional staff and is a section supervisor in the Space Science Instruments Group. He was the program engineer for the Space Telescope Alternate Fine Guidance Sensor program.

Dr. Griffin teaches at the University of Maryland and at The Johns Hopkins University. Prior to joining APL, he worked at Link Division of Singer, Computer Science Corp., and the Jet Propulsion Laboratory.

DAVID G. GRANT (right) received a B.S. degree in electrical engineering from the Bradford Durfee College of Technology in 1959 and an M.A. degree in applied mathematics in 1966 from the University of Maryland. He joined APL in 1959 and worked as an engineer on the Typhon weapons system. Mr. Grant later developed electro-optical signal processing techniques for advanced radar systems. He became associated with APL's biomedical program in 1967 and was principal investigator on a three-dimensional X-ray imaging system that received the IR-100 outstanding engineering development award in 1969.

Mr. Grant worked in the Submarine Technology Division before accepting a university interdivisional appointment to the Johns Hopkins School of Medicine in 1975 as Director of Radiation Therapy Physics. In 1978, he was appointed director of the Division of Clinical Engineering. Mr. Grant returned to full-time duties at APL in 1982 in the Space Department as program manager of the Hubble Space Telescope Fine Guidance Program. Currently, he is program manager of the Polar Bear satellite mission.

Mr. Grant was appointed to the principal professional staff in 1970 and holds the appointments of Associate Professor of Biomedical Engineering and Assistant Professor of Oncology and Radiology in the School of Medicine.

The biographical note on THOMAS E. STRIKWERDA may be found following his article on "The Bird-Borne Transmitter."